Stress intensity factor computation using the method of fundamental solutions: Mixed-mode problems

J. R. Berger[1], Andreas Karageorghis[2] and P. A. Martin[3, *, †]

[1]*Division of Engineering, Colorado School of Mines, Golden, Colorado 80401, U.S.A.*
[2]*Department of Mathematics and Statistics, University of Cyprus, P.O. Box 20537, CY-1678 Nicosia, Cyprus*
[3]*Department of Mathematical and Computer Sciences, Colorado School of Mines, Golden, Colorado 80401, U.S.A.*

SUMMARY

The method of fundamental solutions is applied to the computation of stress intensity factors in linear elastic fracture mechanics. The displacements are approximated by linear combinations of the fundamental solutions of the Cauchy–Navier equations of elasticity and the leading terms for the displacement near the crack tip. Two algorithms are developed, one using a single domain and one using domain decomposition. Numerical results are given. Copyright © 2006 John Wiley & Sons, Ltd.

1. INTRODUCTION

A variety of methods are currently available for computing stress intensity factors (SIFs) for elastic crack problems. The SIF is a measure of the strength of the stress singularity at a crack tip, and is useful from a mechanics perspective as it characterizes the displacement, stress and strain in the near field around the crack tip. Additionally, the stress intensity concept is important in terms of crack extension as critical values of the SIF govern crack initiation.

The calculation of SIFs in finite solids under arbitrary loading conditions is difficult and is usually done through numerical approximation. Typically this is performed using finite element methods [1, 2], boundary element methods [3, 4], or boundary collocation of crack-tip stress-field expansions [5]. For the modelling of crack extensions, boundary-type methods have some advantages over domain discretization methods due to the ease in extending the crack front.

---

*Correspondence to: P. A. Martin, Department of Mathematical and Computer Sciences, Colorado School of Mines, Golden, Colorado 80401, U.S.A.
†E-mail: pamartin@mines.edu

Typical boundary element methods for crack modelling rely on either Green's functions appropriate for crack problems [6, 7] or by using hypersingular integral equations over the crack surfaces [8]. A comprehensive review of SIF computation techniques can be found in Reference [9].

The method of fundamental solutions (MFS) is another boundary-type method; for reviews, with many references, see References [10–13]. The MFS is a mesh-free method in which approximations are expressed in terms of discrete point sources (singularities) applied outside the physical boundary of the solid. These singularities can either have preassigned locations or their locations can be taken as unknowns. In the case when the locations are not preassigned, the satisfaction of the boundary conditions leads to a non-linear least-squares problem. In the case when the locations are preassigned, the imposition of the boundary conditions may be done in a linear least-squares sense or by simple collocation. In this paper, all singularity locations are preassigned and the boundary conditions are imposed in a linear least-squares sense.

The MFS, being a boundary-type technique, is well-suited for dealing with crack problems (and boundary-value problems with boundary singularities in general) for the reasons already mentioned. Further, unlike other boundary-type methods, it avoids numerical integration which could be potentially troublesome, especially in problems involving boundary singularities. Also, it is very easy to implement, and, as the solution of the problem is expressed as a linear combination of fundamental solutions it is natural (and easy) to incorporate the singular behaviour of the singularity into this expansion. However, it should be mentioned that the MFS is not a general purpose method and that it is only (easily) applicable to problems governed by equations for which the fundamental solutions are known.

Recently [14], the MFS has been used for the computation of SIFs in a simple, symmetric situation, in which the loading and geometry were such that a crack on the x-axis ($y = 0$) opened in mode I; the problem is symmetric about the x-axis, and so it is sufficient to treat one half of the physical problem, giving a reduced problem for $y > 0$ with boundary conditions on $y = 0$. In Reference [14], the usual displacement field expansions for the MFS were augmented by the mode I elastic crack tip displacement expansions, thereby allowing the SIF to be treated as simply an additional unknown which is determined upon solution of the least-squares system. The methodology was successfully applied to several opening-mode fracture problems.

Here, we extend the method developed in Reference [14] to problems involving not only the opening mode but the forward shear mode (mode II) as well. The resulting mixed-mode problem is solved numerically using the MFS in two different formulations. The first formulation follows the idea presented in Reference [14] of appending the usual MFS displacement field expansions with the elastic crack tip expansions. However, numerical experiments using this approach indicate some difficulties with deeper cracks. We therefore develop a second formulation using a domain decomposition approach similar to that used in Reference [15] for bimaterial problems; see also Reference [16]. We then use the developed method to calculate SIFs for a variety of crack lengths under mixed-mode loading conditions.

We begin by formulating a plane-strain problem for an oblique edge crack in a rectangular domain; our methods are sufficiently flexible to permit domains of other shapes, although we do assume that the crack is straight. Two MFS formulations are described in Section 3. The simplest, called *monodomain discretization* (Section 3.1), uses fundamental solutions placed outside the physical domain together with the known singular functions for a straight (semi-infinite) crack. We use only the leading-order singular functions, although further terms could be incorporated if desired. In Section 3.2, an approach based on *domain decomposition* is developed. The problem is split in two, using an artificial cut on which continuity conditions are enforced. This method

is more complicated but more accurate, especially for longer cracks. Some numerical results are presented in Section 4 with concluding remarks in Section 5.

2. GOVERNING EQUATIONS

In the absence of body forces, the governing equations of equilibrium for a homogeneous, isotropic, linear-elastic solid are the Cauchy–Navier equations. Using the indicial tensor notation in terms of the displacements u_1, u_2, the Cauchy–Navier equations, in a bounded two-dimensional domain Ω, take the form [17]

$$(\lambda + \mu)u_{k,ki} + \mu u_{i,kk} = 0, \quad i, k = 1, 2 \tag{1}$$

where λ and μ are the Lamé elastic constants. In the system, summation over repeated subscripts is implied and partial derivatives are denoted by a comma. In the linear theory, the strains ε_{ij}, $i, j = 1, 2$, are related to the displacement gradients by means of $\varepsilon_{ij} = (u_{i,j} + u_{j,i})/2$, and the stresses σ_{ij}, $i, j = 1, 2$, are given by Hooke's law $\sigma_{ij} = \lambda \delta_{ij} u_{k,k} + 2\mu\varepsilon_{ij}$. The tractions t_j, $j = 1, 2$ are defined in terms of the stresses as $t_i = \sigma_{ij} n_j$, where n_1 and n_2 denote the co-ordinates of the outward normal to the boundary. Equations (1) are subject to boundary conditions

$$B_i[u_1, u_2, t_1, t_2] = f_i \quad \text{on } \partial\Omega \ i = 1, 2 \tag{2}$$

where $\partial\Omega$ is the boundary of Ω, which we assume to be piecewise smooth, and the operators B_i, $i = 1, 2$, may specify displacement, traction or mixed boundary conditions.

The leading term for the two-dimensional displacement field (v_1, v_2) near the crack tip for plane strain is given by Anderson [18]

$$v_1^S(r, \theta, K_I, K_{II}) = \frac{K_I}{\mu} \sqrt{\frac{r}{2\pi}} \cos\frac{\theta}{2} \left[1 - 2v + \sin^2\frac{\theta}{2}\right] + \frac{K_{II}}{\mu} \sqrt{\frac{r}{2\pi}} \sin\frac{\theta}{2} \left[2 - 2v + \cos^2\frac{\theta}{2}\right] \tag{3}$$

$$v_2^S(r, \theta, K_I, K_{II}) = \frac{K_I}{\mu} \sqrt{\frac{r}{2\pi}} \sin\frac{\theta}{2} \left[2 - 2v - \cos^2\frac{\theta}{2}\right] - \frac{K_{II}}{\mu} \sqrt{\frac{r}{2\pi}} \cos\frac{\theta}{2} \left[1 - 2v - \sin^2\frac{\theta}{2}\right] \tag{4}$$

Here v_1^S and v_2^S are the displacement components corresponding to the axes along the crack and perpendicular to it at the crack tip E, as shown in Figure 1; also, (r, θ) are the polar co-ordinates situated at the crack tip, corresponding to the above (local) axes. The coefficients K_I and K_{II} are the mode I and mode II SIFs, respectively, and v is Poisson's ratio. From Figure 1, it follows that if (x_1, x_2) are the horizontal and vertical co-ordinates of a point with respect to the origin O, then

$$x_1 = a\cos\beta + r\cos(\theta + \beta), \quad x_2 = a\sin\beta + r\sin(\theta + \beta) \tag{5}$$

and

$$r = \sqrt{(x_1 - a\cos\beta)^2 + (x_2 - a\sin\beta)^2}, \quad \tan(\theta + \beta) = \frac{x_2 - a\sin\beta}{x_1 - a\cos\beta} \tag{6}$$

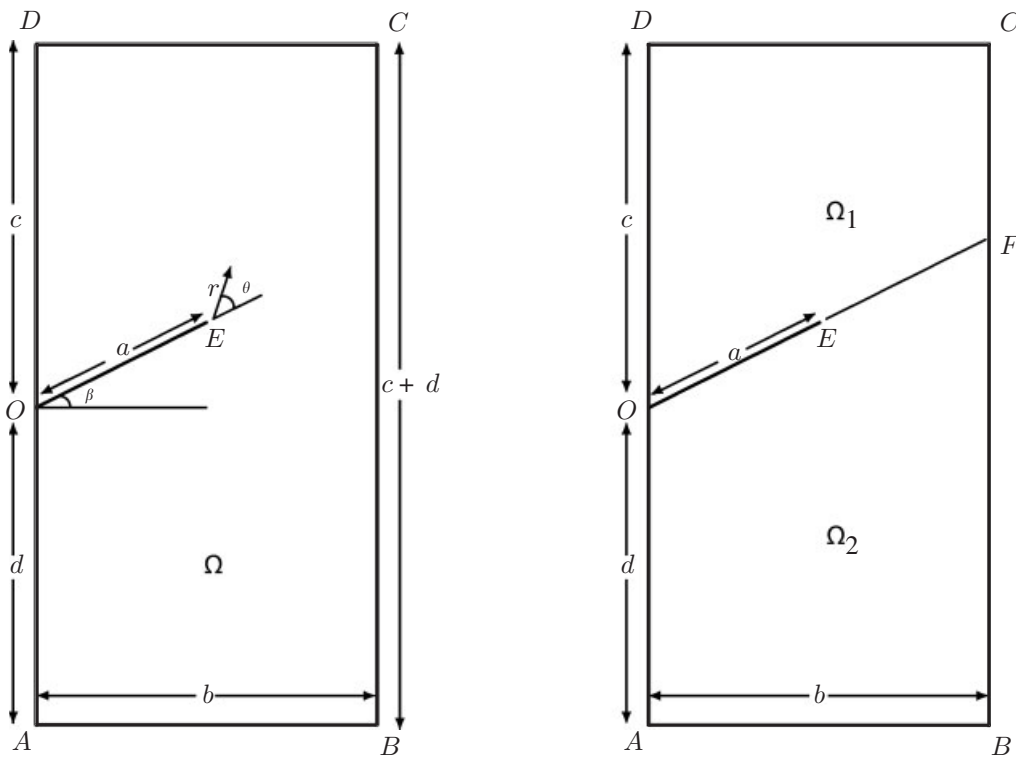Figure 1. An oblique edge crack in a plate Ω. The left-hand diagram shows the local polar co-ordinates at the crack tip, E. The right-hand diagram shows the domain decomposition, using the line EF.

Therefore, for a point with co-ordinates (x_1, x_2), the displacements u_1^S and u_2^S corresponding to the horizontal and vertical co-ordinates with respect to the origin O are given by

$$u_1^S(x_1, x_2, K_{\mathrm{I}}, K_{\mathrm{II}}) = v_1^S(r, \theta, K_{\mathrm{I}}, K_{\mathrm{II}}) \cos \beta - v_2^S(r, \theta, K_{\mathrm{I}}, K_{\mathrm{II}}) \sin \beta \qquad (7)$$

and

$$u_2^S(x_1, x_2, K_{\mathrm{I}}, K_{\mathrm{II}}) = v_1^S(r, \theta, K_{\mathrm{I}}, K_{\mathrm{II}}) \sin \beta + v_2^S(r, \theta, K_{\mathrm{I}}, K_{\mathrm{II}}) \cos \beta \qquad (8)$$

In addition to the displacement field, we will also require the tractions associated with the crack-tip stress field for implementing the MFS. The near-field stresses at the tip of a crack are given by Anderson [18]

$$\sigma_{11}(r, \theta, K_{\mathrm{I}}, K_{\mathrm{II}}) = \frac{K_{\mathrm{I}}}{\sqrt{2\pi r}} \cos \frac{\theta}{2} \left[1 - \sin \frac{\theta}{2} \sin \frac{3\theta}{2} \right] - \frac{K_{\mathrm{II}}}{\sqrt{2\pi r}} \sin \frac{\theta}{2} \left[2 + \cos \frac{\theta}{2} \cos \frac{3\theta}{2} \right] \qquad (9)$$

$$\sigma_{12}(r, \theta, K_{\mathrm{I}}, K_{\mathrm{II}}) = \frac{K_{\mathrm{I}}}{\sqrt{2\pi r}} \cos \frac{\theta}{2} \sin \frac{\theta}{2} \cos \frac{3\theta}{2} + \frac{K_{\mathrm{II}}}{\sqrt{2\pi r}} \cos \frac{\theta}{2} \left[1 - \sin \frac{\theta}{2} \sin \frac{3\theta}{2} \right] \qquad (10)$$

$$\sigma_{22}(r, \theta, K_{\mathrm{I}}, K_{\mathrm{II}}) = \frac{K_{\mathrm{I}}}{\sqrt{2\pi r}} \cos\frac{\theta}{2}\left[1 + \sin\frac{\theta}{2}\sin\frac{3\theta}{2}\right] + \frac{K_{\mathrm{II}}}{\sqrt{2\pi r}}\sin\frac{\theta}{2}\cos\frac{\theta}{2}\cos\frac{3\theta}{2} \quad (11)$$

where the local crack-tip co-ordinates (r, θ) are related to the global (x_1, x_2) co-ordinates via (6). Given a local normal vector (n_1, n_2) in the (x_1, x_2) co-ordinates, the components of the traction vector (t_1, t_2) in the (x_1, x_2) co-ordinates are then given by

$$t_1(x_1, x_2, K_{\mathrm{I}}, K_{\mathrm{II}}) = \sigma_{11}(n_1\cos^2\beta + n_2\sin\beta\cos\beta) + \sigma_{22}(n_1\sin^2\beta - n_2\sin\beta\cos\beta)$$
$$+ \sigma_{12}(-n_1\sin 2\beta + n_2\cos 2\beta) \quad (12)$$

$$t_2(x_1, x_2, K_{\mathrm{I}}, K_{\mathrm{II}}) = \sigma_{11}(n_1\cos\beta\sin\beta + n_2\sin^2\beta) + \sigma_{22}(-n_1\cos\beta\sin\beta + n_2\cos^2\beta)$$
$$+ \sigma_{12}(n_1\cos 2\beta + n_2\sin 2\beta) \quad (13)$$

3. MFS FORMULATIONS

3.1. Monodomain discretization

In this formulation, the displacements at a point P in region Ω, are approximated by u_{1_N}, u_{2_N} as linear combinations of fundamental solutions and expressions (3) and (4):

$$u_{1_N}(K_{\mathrm{I}}^N, K_{\mathrm{II}}^N, \mathbf{a}, \mathbf{b}, \mathbf{Q}; P) = u_1^S(x_{1_P}, x_{2_P}, K_{\mathrm{I}}^N, K_{\mathrm{II}}^N)$$
$$+ \sum_{j=1}^N a_j G_{11}(P, Q_j) + \sum_{j=1}^N b_j G_{12}(P, Q_j) \quad (14)$$

$$u_{2_N}(K_{\mathrm{I}}^N, K_{\mathrm{II}}^N, \mathbf{a}, \mathbf{b}, \mathbf{Q}; P) = u_2^S(x_{1_P}, x_{2_P}, K_{\mathrm{I}}^N, K_{\mathrm{II}}^N)$$
$$+ \sum_{j=1}^N a_j G_{21}(P, Q_j) + \sum_{j=1}^N b_j G_{22}(P, Q_j) \quad (15)$$

and the tractions are approximated accordingly [15]. Here, (x_{1_P}, x_{2_P}) denote the co-ordinates of the point P. The $2N$-vector $\mathbf{Q}$ contains the co-ordinates of the N singularities surrounding region Ω, while $\mathbf{a} = (a_1, a_2, \ldots, a_N)$ and $\mathbf{b} = (b_1, b_2, \ldots, b_N)$ are vectors containing unknown coefficients. Also, K_{I}^N, K_{II}^N are the (unknown) approximations to the SIFs K_{I} and K_{II}. The functions G_{11}, G_{12}, G_{21} and G_{22} are the fundamental solutions of the system (1). For a singularity located at Q acting on P they are (see, for example, References [19, 17])

$$G_{11}(P, Q) = -\frac{1}{8\pi\mu(1-v)}\left[(3-4v)\log r_{PQ} - \frac{(x_{1_P} - x_{1_Q})^2}{r_{PQ}^2}\right] \quad (16)$$

$$G_{12}(P, Q) = G_{21}(P, Q) = \frac{1}{8\pi\mu(1-v)}\left[\frac{(x_{1_P} - x_{1_Q})(x_{2_P} - x_{2_Q})}{r_{PQ}^2}\right] \quad (17)$$

$$G_{22}(P, Q) = -\frac{1}{8\pi\mu(1-v)}\left[(3-4v)\log r_{PQ} - \frac{(x_{2_P} - x_{2_Q})^2}{r_{PQ}^2}\right] \quad (18)$$

where $r_{PQ} = \sqrt{(x_{1_P} - x_{1_Q})^2 + (x_{2_P} - x_{2_Q})^2}$ and (x_{1_Q}, x_{2_Q}) are the co-ordinates of the point Q.

In the linear least-squares MFS, the co-ordinates of the singularities Q_j are prescribed. If the boundary of Ω is denoted by $\partial\Omega = AB \cup BC \cup CD \cup DA$ (see Figure 1), these are located on a *pseudoboundary* $\partial\tilde{\Omega}$, similar to $\partial\Omega$ and at a distance e from it. The pseudoboundary does not contain a crack. A set of points $\{P_i\}_{i=1}^M$ is selected on $\partial\Omega \cup OE$. In particular, we take M_{AB}, M_{BC}, M_{CD} and M_{DA} uniformly distributed points on the segments AB, BC, CD and DA, respectively. Finally, M_{OE} points are placed on OE, thus $M_{AB} + M_{BC} + M_{CD} + M_{DA} + M_{OE} = M$. Also, N_{AB}, N_{BC}, N_{CD} and N_{DA} singularities are placed on segments parallel to AB, BC, CD and DA, respectively. Thus $N_{AB} + N_{BC} + N_{CD} + N_{DA} = N$. The $2N + 2$ coefficients $\mathbf{a}$, $\mathbf{b}$, K_{I}^N and K_{II}^N are determined from the satisfaction of the boundary conditions:

$$B_1[u_{1_N}, u_{2_N}, t_{1_N}, t_{2_N}](K_{\mathrm{I}}^N, K_{\mathrm{II}}^N, \mathbf{a}, \mathbf{b}, \mathbf{Q}; P_i) = f_1(P_i)$$
$$B_2[u_{1_N}, u_{2_N}, t_{1_N}, t_{2_N}](K_{\mathrm{I}}^N, K_{\mathrm{II}}^N, \mathbf{a}, \mathbf{b}, \mathbf{Q}; P_i) = f_2(P_i), \quad i = 1, 2, \ldots, M \quad (19)$$

System (19) is a linear system of $2M$ equations in $2N + 2$ unknowns. In this study, we choose $M > N + 1$ and the resulting system is overdetermined. This system is solved in a least-squares sense using the NAG [20] routine F04AMF which uses a *QR* factorization and iterative refinement.

3.2. Domain decomposition

The domain Ω is now subdivided into two subdomains Ω_1 and Ω_2 as shown in Figure 1. The displacements $u_{1_N}^{(\ell)}, u_{2_N}^{(\ell)}$ at a point P in region Ω_ℓ, $\ell = 1, 2$, are approximated by

$$u_{1_N}^{(\ell)}(K_{\mathrm{I}}^N, K_{\mathrm{II}}^N, \mathbf{a}^{(\ell)}, \mathbf{b}^{(\ell)}, \mathbf{Q}^{(\ell)}; P) = u_1^S(x_{1_P}, x_{2_P}, K_{\mathrm{I}}^N, K_{\mathrm{II}}^N)$$
$$+ \sum_{j=1}^N a_j^{(\ell)} G_{11}(P, Q_j^{(\ell)}) + \sum_{j=1}^N b_j^{(\ell)} G_{12}(P, Q_j^{(\ell)}) \quad (20)$$

$$u_{2_N}^{(\ell)}(K_{\mathrm{I}}^N, K_{\mathrm{II}}^N, \mathbf{a}^{(\ell)}, \mathbf{b}^{(\ell)}, \mathbf{Q}^{(\ell)}; P) = u_2^S(x_{1_P}, x_{2_P}, K_{\mathrm{I}}^N, K_{\mathrm{II}}^N)$$
$$+ \sum_{j=1}^N a_j^{(\ell)} G_{21}(P, Q_j^{(\ell)}) + \sum_{j=1}^N b_j^{(\ell)} G_{22}(P, Q_j^{(\ell)}) \quad (21)$$

with the tractions approximated accordingly.

From Figure 1, it is clear that Ω_1 has boundary $\partial\Omega_1 = OE \cup EF \cup FC \cup CD \cup DO$. The singularities Q_j^1 are located on a pseudoboundary $\partial\tilde{\Omega}_1$, similar to $\partial\Omega_1$ and at a distance e from it. A set of points $\{P_i^1\}_{i=1}^{M_1}$ is selected on $\partial\Omega_1$. In particular, we take M_{OE}, M_{EF}, M_{FC}, M_{CD} and M_{DO} uniformly distributed points on the segments OE, EF, FC, CD and DO, respectively.

Similarly, the singularities $\{Q_j^1\}_{j=1}^{N_1}$ are placed on $\partial\tilde{\Omega}_1$ accordingly, by taking N_{OE}, N_{EF}, N_{FC}, N_{CD} and N_{DO} uniformly distributed singularities on segments parallel to OE, EF, FC, CD and DO, respectively. Clearly, $M_1 = M_{OE} + M_{EF} + M_{FC} + M_{CD} + M_{DO}$ and $N_1 = N_{OE} + N_{EF} + N_{FC} + N_{CD} + N_{DO}$.

In a similar fashion, the singularities Q_j^2 are located on a pseudoboundary $\partial\tilde{\Omega}_2$, similar to $\partial\Omega_2 = OE \cup EF \cup FB \cup BA \cup AO$ and at a distance e from it. In particular, a set of points $\{P_i^2\}_{i=1}^{M_2}$ is selected on $\partial\Omega_2$, and the singularities $\{Q_j^2\}_{j=1}^{N_2}$ are placed on $\partial\tilde{\Omega}_2$ with, analogously to Ω_1, $M_2 = M_{OE} + M_{EF} + M_{FB} + M_{BA} + M_{AO}$ and $N_2 = N_{OE} + N_{EF} + N_{FB} + N_{BA} + N_{AO}$.

The total number of boundary points is therefore $M_1 + M_2$ and the total number of singularities is $N_1 + N_2$. We impose the boundary conditions (19) on the segments OE, FC, CD and DO in Ω_1 and on the segments OE, FB, BA and AO in Ω_2. On the interface EF we impose the continuity conditions

$$u_{jN}^{(1)} = u_{jN}^{(2)} \quad \text{and} \quad t_{jN}^{(1)} + t_{jN}^{(2)} = 0, \quad j = 1, 2 \tag{22}$$

We thus have $2M_1 + 2M_2$ equations in the $2N_1 + 2N_2 + 2$ unknowns $\mathbf{a}^{(\ell)}$, $\mathbf{b}(\ell)$, $\ell = 1, 2$ and K_I^N, K_{II}^N. If we take $M_1 + M_2 > N_1 + N_2 + 1$ the resulting system is overdetermined and, as before, is solved using the NAG routine F04AMF.

3.3. Implementational considerations

In all the examples considered in this study, for simplicity, in the monodomain case, we took $M_{AB} = M_{CD} = M_{OE} = m$ and $M_{BC} = M_{DA} = 2m$ and thus $M = 7m$. Similarly, we took $N_{AB} = N_{CD} = n$ and $N_{BC} = N_{DA} = 2n$ and thus $N = 6n$. Thus we need to solve a linear system of $14m$ equations in $12n + 2$ unknowns. Similarly, in the domain decomposition formulation, we took $M_{OE} = M_{EF} = M_{FC} = M_{CD} = M_{DO} = M_{FB} = M_{BA} = M_{AO} = m$ and $N_{OE} = N_{EF} = N_{FC} = N_{CD} = N_{DO} = N_{FB} = N_{BA} = N_{AO} = n$. Thus $M_1 = M_2 = 5m$, $N_1 = N_2 = 5n$ and we need to solve a linear system of $20m$ equations in $20n + 2$ unknowns.

Our goal is the evaluation of the quantities K_I^N and K_{II}^N. In each problem we considered we took a sequence of values of e, namely $e = 0.01 + 0.01\kappa$, $\kappa = 1, \ldots, 199$ so that $0 < e \leqslant 2$. For each κ, we calculated $K_I^{N(\kappa)}$ and $K_{II}^{N(\kappa)}$. We also calculated the quantities

$$R^{(\kappa)} = \sqrt{[(K_I^{N(\kappa+1)} - K_I^{N(\kappa)})/K_I^{N(\kappa)}]^2 + [(K_{II}^{N(\kappa+1)} - K_{II}^{N(\kappa)})/K_{II}^{N(\kappa)}]^2}$$

The optimal values of K_I^N and K_{II}^N were chosen to be those for which the value of $R^{(\kappa)}$ was minimal. In the case of perpendicular edge cracks ($\beta = 0$), we only considered $K_I^{N(\kappa)}$.

4. NUMERICAL EXAMPLES

We consider an oblique edge crack of length a in a rectangular sheet of width b as shown in Figure 1. The crack angle is β. The governing equations are the equilibrium equations (1), subject
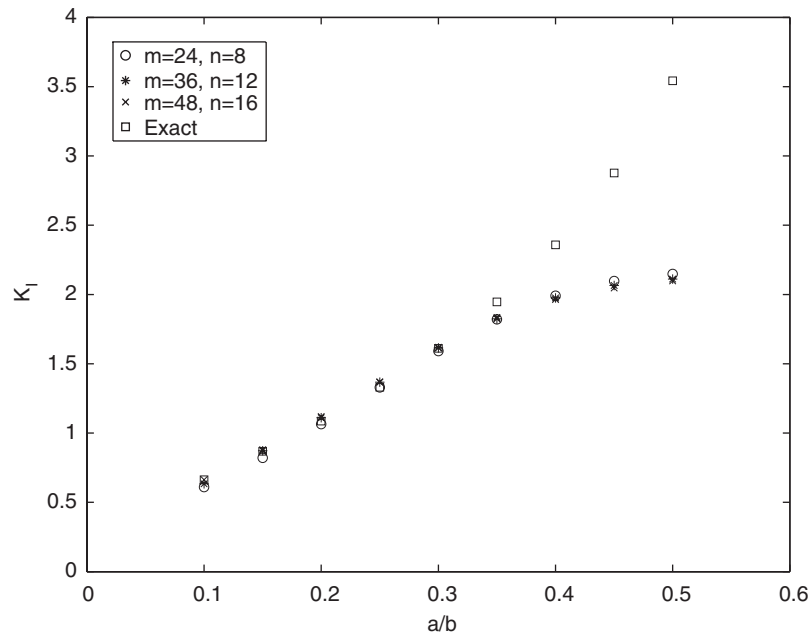
Figure 2. Comparison of K_I using the monodomain discretization for various values of a/b.
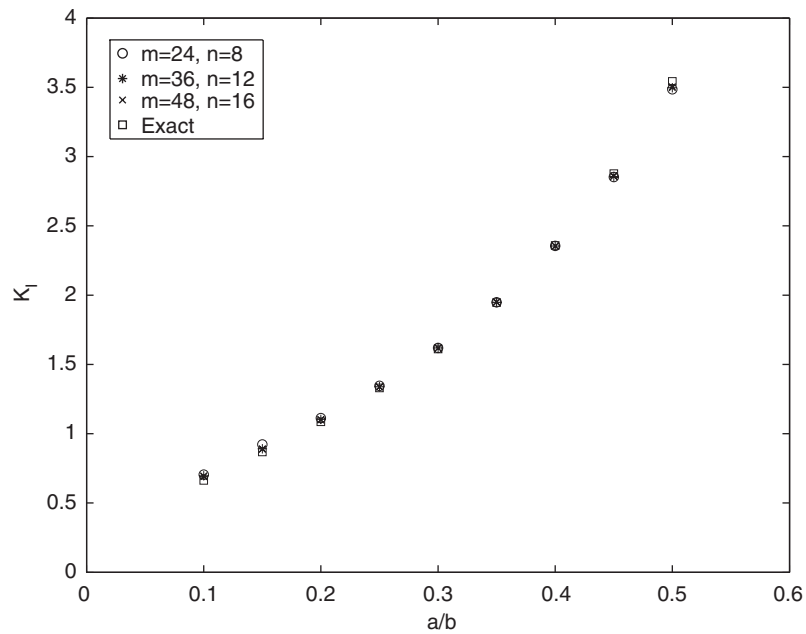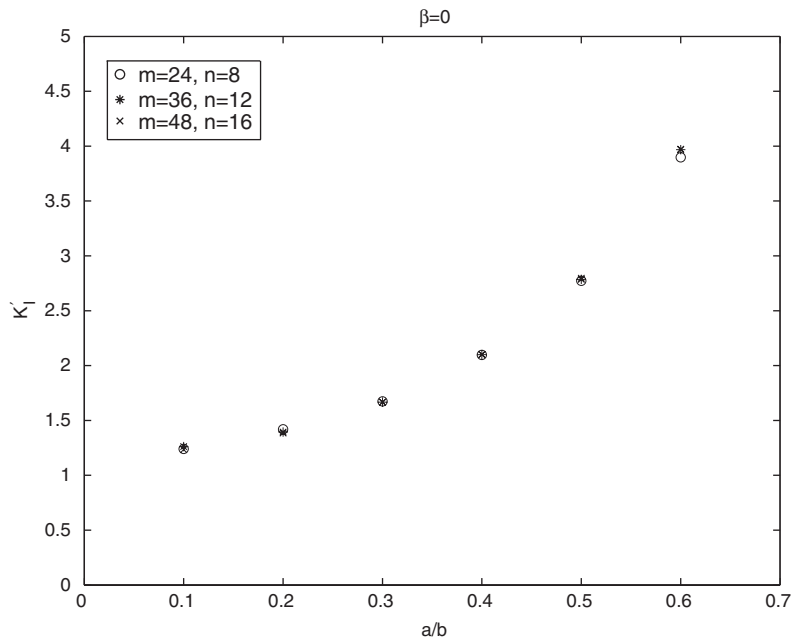

Figure 3. Comparison of K_I using domain decomposition for various values of a/b.

Table I. Values of e optimizing $R^{(\kappa)}$ in Example 1.

m, n	$e = 0.1$	$e = 0.2$	$e = 0.3$	$e = 0.4$	$e = 0.5$
24, 8	0.51	0.28	0.50	0.31	0.48
36, 12	0.14	0.22	0.18	0.36	0.27
48, 16	0.12	0.18	0.25	0.31	0.26

Figure 4. Normalized mode I stress intensity factor for $\beta = 0$.

to the following boundary conditions:

$$
\begin{aligned}
t_1 &= 0, & t_2 &= 0 & &\text{on } DA \\
t_1 &= 0, & t_2 &= 1 & &\text{on } CD \\
t_1 &= 0, & t_2 &= 0 & &\text{on } BC \\
t_1 &= 0, & t_2 &= -1 & &\text{on } AB \\
t_1 &= 0, & t_2 &= 0 & &\text{on } OE
\end{aligned}
\tag{23}
$$

To ensure a unique solution we also impose the following crack-tip condition:

$$
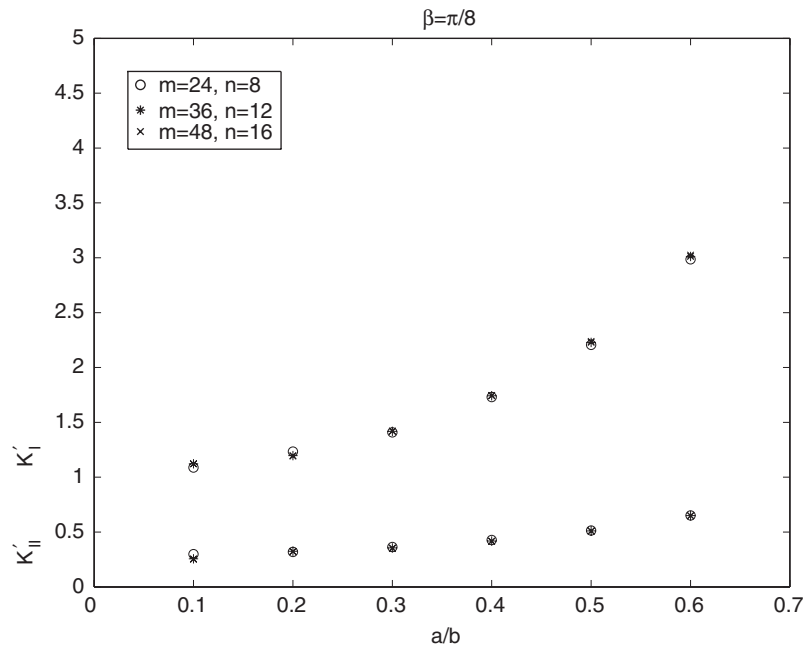u_1 = 0, \quad u_2 = 0 \quad \text{at } E
\tag{24}
$$

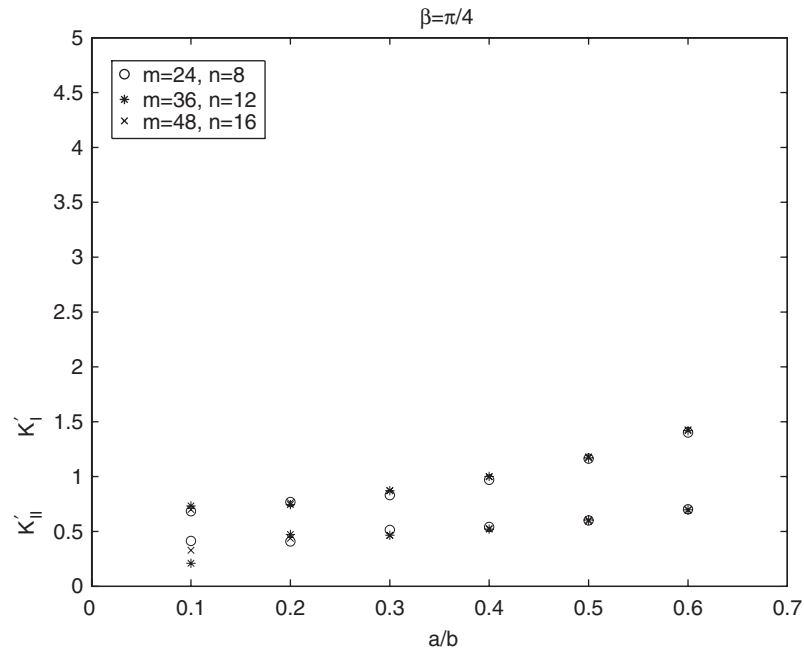Figure 5. Normalized mode I and II stress intensity factors for $\beta = \pi/8$.

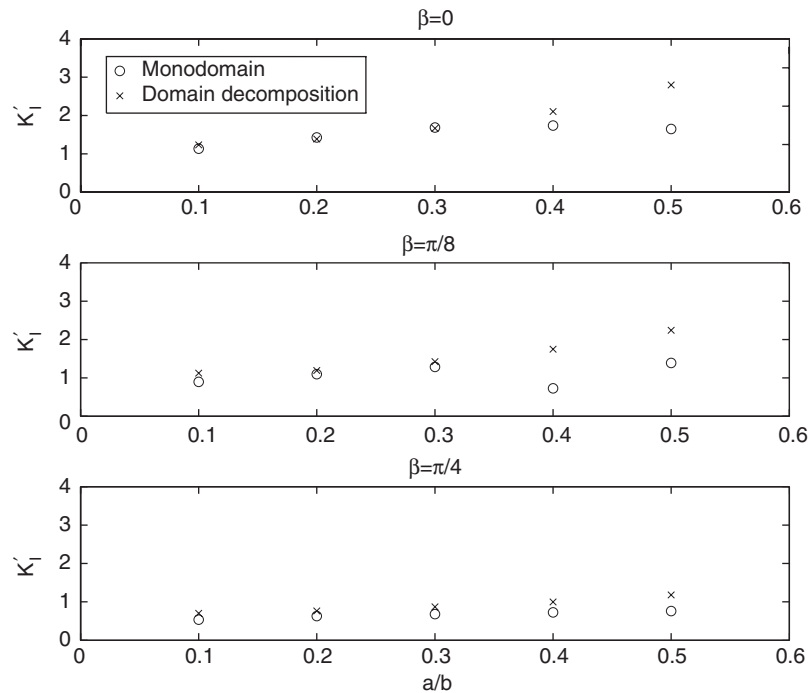Figure 6. Normalized mode I and II stress intensity factors for $\beta = \pi/4$.

Figure 7. Comparison of normalized mode I stress intensity factors, computed using the monodomain discretization and domain decomposition methods.

4.1. Example 1. Perpendicular edge crack

In order to test the methods described in this paper, we first consider the example of a perpendicular edge crack ($\beta = 0$) with $b = 1$ and $c = d = b$. The solution of this (symmetric) problem is known, and is given by the following formula [21, 22]:

$$K_I = \sqrt{\pi a}[1.12 - 0.231(a/b) + 10.55(a/b)^2 - 21.72(a/b)^3 + 30.39(a/b)^4]$$

Clearly, by symmetry, $K_{II} = 0$.

We solved this problem using both the monodomain and the domain decomposition discretizations for different values of m and n and a variety of crack lengths a. In Figures 2 and 3 we present some results for K_I^N for the monodomain and the domain decomposition discretizations, respectively. The approximations in the monodomain discretization are accurate for smaller values of the crack lengths a whereas the approximations in the domain decomposition discretization are accurate for all values of a considered.

In Table I, we present the values of e giving the optimal values of $R^{(\kappa)}$ for various numbers of degrees of freedom and different crack lengths in the case of the domain decomposition discretization.
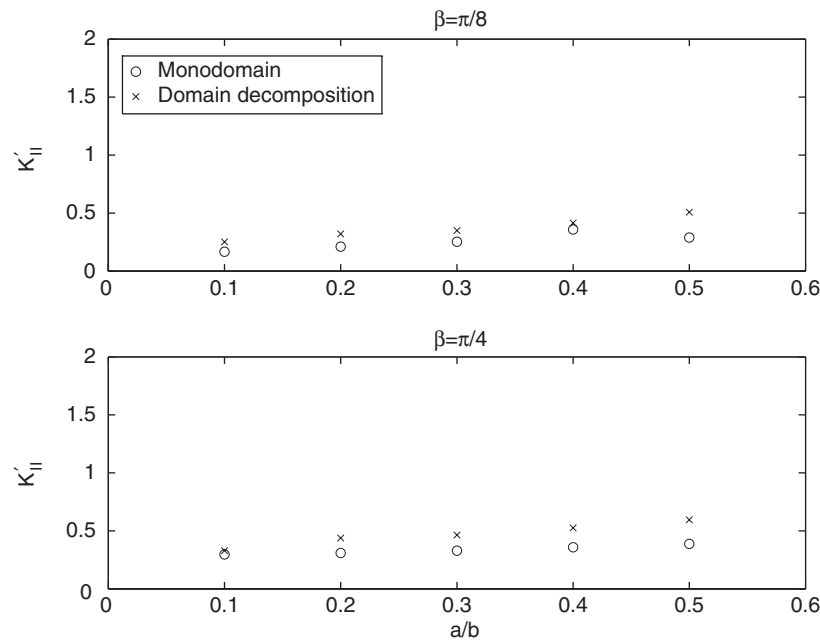
Figure 8. Comparison of normalized mode II stress intensity factors, computed using the monodomain discretization and domain decomposition methods.

4.2. Example 2. Oblique edge crack

We considered the case of a crack at an angle β, with $b = 1$, $c = 3b/2$ and $d = b$. In particular, we considered the angles $\beta = 0$, $\pi/8$ and $\pi/4$. For comparison purposes we shall be presenting the normalized values $K'_I = K^N_I / \sqrt{a\pi}$ and $K'_{II} = K^N_{II} / \sqrt{a\pi}$. In Figures 4–6 we present the domain decomposition computed values of K'_I and K'_{II} for three sets of m and n, for $a = 0.1, 0.2, 0.3, 0.4, 0.5$ and 0.6, for the cases $\beta = 0$, $\beta = \pi/8$ and $\beta = \pi/4$, respectively. These results indicate consistency for various numbers of degrees of freedom. Further, the results for $a = 0.3, 0.4, 0.5$ and 0.6 are in excellent agreement with the results of Wilson, as given in Reference [4, Figure 6.21] (results for $a < 0.3$ are not given in Reference [4]).

Also, in Figures 7 and 8, we compare the results obtained with the monodomain and the domain decomposition discretizations for the case when $m = 48$, $n = 16$, for K'_I and K'_{II}, respectively. The two sets of results agree for smaller values of a and, as in Example 1, the monodomain discretization suffers from loss of accuracy as a increases. It should be mentioned that in the case $a = 0.1$ for $m = 48$, $n = 16$, in some instances, in the domain decomposition discretization, the iterative refinement used in the least-squares method failed to converge, indicating that the coefficient matrix in the MFS system is too ill-conditioned. This problem was overcome by reducing the number of sources used.

Finally, in Figure 9 we present the variation of K'_I and K'_{II} with the distance e of the pseudoboundary from the boundary in the domain decomposition discretization. This behaviour is typical of both methods considered.
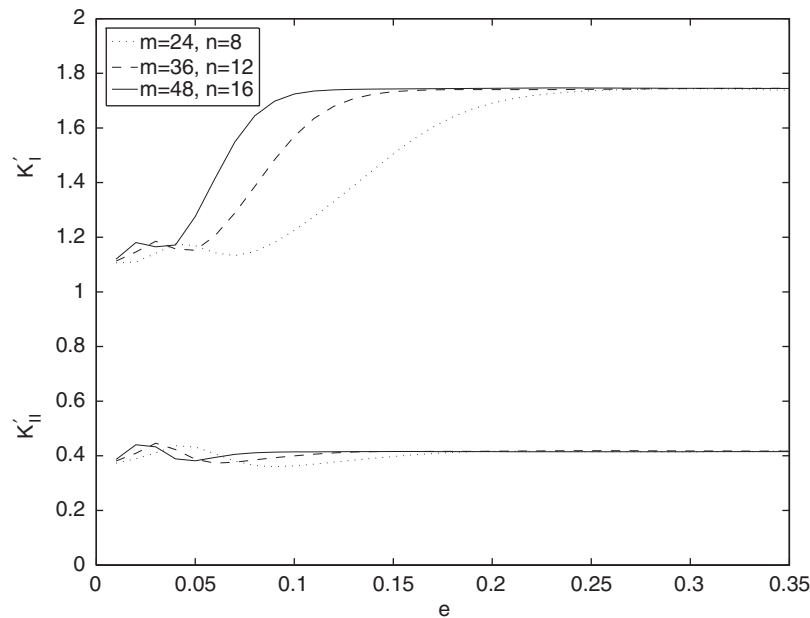
Figure 9. Variation of normalized mode I and II stress intensity factors with *e*.

5. CONCLUDING REMARKS

Two applications of the MFS have been described, in the context of plane-strain elastostatics. Both are applicable to straight edge cracks in bounded regions; the outer boundary can have any shape. The main virtue of the first method (monodomain discretization) is its simplicity: the basic MFS is augmented by a singular function to take account of the crack-tip singularity. The method was shown to give good results for short cracks. This result can be explained as follows. The crack opening displacement (the discontinuity in the vector (u_1, u_2) across the crack) is represented by

$$\frac{4(1-v)}{\mu}\sqrt{\frac{r}{2\pi}}\,(K_{\mathrm{II}}\cos\beta - K_{\mathrm{I}}\sin\beta,\ K_{\mathrm{II}}\sin\beta + K_{\mathrm{I}}\cos\beta) \quad \text{for } 0 < r < a$$

this approximation is only expected to be accurate near $r = 0$. Increasing N (the number of fundamental solutions) will not lead to improvements because any linear combination of fundamental solutions will be continuous across the crack. Of course, we could augment the approximations with additional higher-order crack-tip solutions (proportional to $r^{n+1/2}$ with $n = 1, 2, \ldots$) but this would make the method more complicated. Thus, the simplest monodomain discretization, as described in this study, should only be used for short cracks.

The second method utilized domain decomposition. Such splitting (sometimes called 'stitching') has been used before for crack problems, using boundary element methods [23, 24]. As a result, the crack has two faces, and the displacement near one face (in Ω_1, say; see Figure 1) can be represented by fundamental solutions near the other face (in Ω_2): the numerical approximation can be improved by increasing N. Consequently, better results are obtained, especially for longer cracks.

In the present study, in order to demonstrate its applicability, the MFS is applied to test problems from the literature. However, the method could be applied to more complicated geometries and problems with multiple cracks of various shapes. Further extensions are feasible, including straight cracks with two tips and anisotropic media. Additional internal boundaries can also be treated without difficulty; applications to cracks starting from holes are of interest. Furthermore, applications to Signorini-type problems are envisaged, in which crack faces may come into contact along part of their length as the loading is changed. Some of these extensions are currently under consideration.

REFERENCES

1. Barsoum RS. On the use of isoparametric finite elements in linear fracture mechanics. *International Journal for Numerical Methods in Engineering* 1976; **10**:25–37.
2. Pu SL, Hussain MA, Lorenson WE. The collapsed cubic isoparametric element as a singular element for crack problems. *International Journal for Numerical Methods in Engineering* 1978; **12**:1727–1742.
3. Cruse TA. *Boundary Element Analysis in Computational Fracture Mechanics*. Kluwer: Dordrecht, 1988.
4. Aliabadi MH, Rooke DP. *Numerical Fracture Mechanics*. Computational Mechanics Publications: Boston, 1991.
5. Srawley JE, Gross B. Stress intensity factors for crackline loaded edge crack specimens. *Materials Research and Standards* 1967; **7**:155–162.
6. Snyder MD, Cruse TA. Boundary-integral equation analysis of cracked anisotropic plates. *International Journal of Fracture* 1975; **11**:315–328.
7. Berger JR, Tewary VK. Boundary integral equation formulation for interface cracks in anisotropic materials. *Computational Mechanics* 1997; **20**:261–266.
8. Martin PA, Rizzo FJ. On boundary integral equations for crack problems. *Proceedings of the Royal Society A* 1989; **421**:341–355.
9. Atluri SN (ed.). *Computational Methods in the Mechanics of Fracture*. Elsevier: Amsterdam, 1986.
10. Fairweather G, Karageorghis A. The method of fundamental solutions for elliptic boundary value problems. *Advances in Computational Mathematics* 1998; **9**:69–95.
11. Golberg MA, Chen CS. The method of fundamental solutions for potential, Helmholtz and diffusion problems. In *Boundary Integral Methods and Mathematical Aspects*, Golberg MA (ed.). WIT Press/Computational Mechanics Publications: Boston, 1999; 103–176.
12. Fairweather G, Karageorghis A, Martin PA. The method of fundamental solutions for scattering and radiation problems. *Engineering Analysis with Boundary Elements* 2003; **27**:759–769.
13. Cho HA, Golberg MA, Muleshkov AS, Li X. Trefftz methods for time dependent partial differential equations. *Computers, Materials and Continua* 2004; **1**:1–37.
14. Karageorghis A, Poullikkas A, Berger JR. Stress intensity factor computation using the method of fundamental solutions. *Computational Mechanics* 2006; **37**:445–454.
15. Berger JR, Karageorghis A. The method of fundamental solutions for layered elastic materials. *Engineering Analysis with Boundary Elements* 2001; **25**:877–886.
16. Fenner RT. A force field superposition approach to plane elastic stress and strain analysis. *Journal of Strain Analysis for Engineering Design* 2001; **36**:517–529.
17. Hartmann F. Elastostatics. In *Progress in Boundary Element Methods*, Brebbia CA (ed.), vol. 1. Pentech Press: Plymouth, 1981; 84–167.
18. Anderson TL. *Fracture Mechanics: Fundamentals and Applications*. CRC Press: Boca Raton, FL, 1995.
19. Banerjee PK, Butterfield R. *Boundary Element Methods in Engineering Science*. McGraw-Hill: New York, 1981.

20. Numerical Analysis Group (NAG) Library Mark 20, NAG Ltd, Wilkinson House, Jordan Hill Road, Oxford, U.K., 2001.
21. Shah SP, Swartz SE, Ouyang C. *Fracture Mechanics of Concrete*: *Applications of Fracture Mechanics to Concrete, Rock and Other Quasi-Brittle Materials*. Wiley: New York, 1995.
22. Tada H, Paris P, Irwin G. *The Stress Analysis of Cracks Handbook* (2nd edn). Paris Productions Inc., 1985.
23. Blandford GE, Ingraffea AR, Liggett JA. Two-dimensional stress intensity factor computations using the boundary element method. *International Journal for Numerical Methods in Engineering* 1981; **17**:387–404.
24. Jia ZH, Shippy DJ, Rizzo FJ. On the computation of two-dimensional stress intensity factors using the boundary element method. *International Journal for Numerical Methods in Engineering* 1988; **26**:2739–2753.